Supporting Information

Self-Organized 3D Porous Graphene Dual-Doped with Biomass-Sponsored Nitrogen and Sulfur for Oxygen Reduction and Evolution

Ibrahim Saana Amiinu,[†] Jian Zhang,[†] Zongkui Kou,[†] Xiaobo Liu,[†] Owusu Kwadwo Asare,[‡] Huang Zhou,[†] Kun Cheng,[†] Haining Zhang,[†] Liqiang Mai,[†‡] Mu Pan,[†] and Shichun Mu[†,*]

[†] State Key Laboratory of Advanced Technology for Materials Synthesis and Processing, Wuhan University of Technology, Wuhan 430070, P. R. China

[‡] WUT–Harvard Joint Nano Key Laboratory, Wuhan University of Technology, Wuhan 430070, China

* Corresponding author: Tel: +86 27 87651837, E-mail: msc@whut.edu.cn

Supplementary Methods and Figures

Physicochemical Characterization

TEM images were obtained from a JEM–2010FEF high resolution electron microscope operated at 20 kV. X-ray diffraction (XRD) patterns were recorded on a Rigaku D/MAX-RB diffractometer with monochromatized Cu-Kα radiation at 50 mA and 40 kV. Surface features and morphologies were investigated using a JSM–7100F field emission scanning electron microscopy (FE-SEM) installed with an energy dispersive analyzer and operated at 20 kV. Selected area elemental mapping was obtained via Energy-dispersive X-ray Spectroscopy (EDX). Atomic force microscopic (AFM) images were acquired under tapping mode on a Si-tip NanoScope IIIA, Digital Instruments/VEECO. A Fourier transform infrared (FT-IR) spectrometer (Bio-Rad FTS 300) was used to recorded IR spectra of solid particles by KBr pellet method. Raman spectra were analyzed on a LabRAM Aramis Raman equipment using Ar-ion laser at λ=632.8 nm. A VG Multi-lab 2000 instrument was used to acquire X-ray photoelectron spectroscopic (XPS) data. Elemental composition was performed on a German elemental analysis instrument (GmbH EL Cube Vario Elemental Analyzer), and nitrogen sorption porosimetry on a Micromeritics TriStar II 3020, Version 2.00. The yield per sample was determined by weight-difference analysis of the initial (GO/Hn and GO/L-Cysteine mixtures) and final (NSG) samples.

Electrochemical Characterization

A catalyst-ink was prepared by ultra-sonically dispersing 5.0 mg of catalyst in a solution of Nafion (5 wt.%, DuPont)/UHP water/isopropanol and optimized for homogeneous dispersion. The working electrode was prepared by loading the catalyst-ink (10 μL) onto a glassy carbon electrode

(0.196 cm^2) and dried under constant rotation at 600 rpm for at least 20 min under ambient conditions. Commercial Pt/C (20 wt.%, 20 µg Pt cm^{-2}) was used as a benchmark. A saturated calomel electrode (SCE) and platinum wire were used as reference and counter electrodes, respectively. All electrochemical properties were measured on a three electrode electrochemical system (CHI-660E) at room temperature. Linear sweep voltammetry (LSV) was measured by rotating disk electrode technique using a Pine research instrument, USA, at the scan rate of 5 mVs^{-1} vs SCE at 1600 rpm in 0.1 M KOH and 0.1 M $HClO_4$. Cyclic voltammograms (CV) was recorded at the scan rate of 20 mVs^{-1} vs SCE. The oxygen evolution reaction (OER) properties were also characterized in 0.1 M KOH at a scan rate of 5 mVs^{-1}, and the electro-potential for water oxidation evaluated at 10 $mAcm^{-2}$ current density ($E_{j=10}$). The ORR stability and tolerance were evaluated by chronoamperometry (current vs time) at -0.3 V and 1600 rpm. The resistance to CO (O_2 + CO, $V_{CO}/V_{O2} \approx$ 10 %) contamination and methanol (O_2 + 1 M CH_3OH) oxidation molecules was also probed in both media. The half-wave potential ($E_{1/2}$) was estimated as the potential half-way (50 %) between zero current and the estimated diffusion-limited current density (j_L) at the specified potential of -1.0V, and onset-potential (E_o) as the potential at which the ORR current was ~5 % of the estimated diffusion-limited current density. The working electrode was electrochemically cleansed and stabilized via potential cycling at 0.5 Vs^{-1} for 100 cycles. The average number of electrons transferred was estimated using the Koutecky-Levich (K–L) equation.

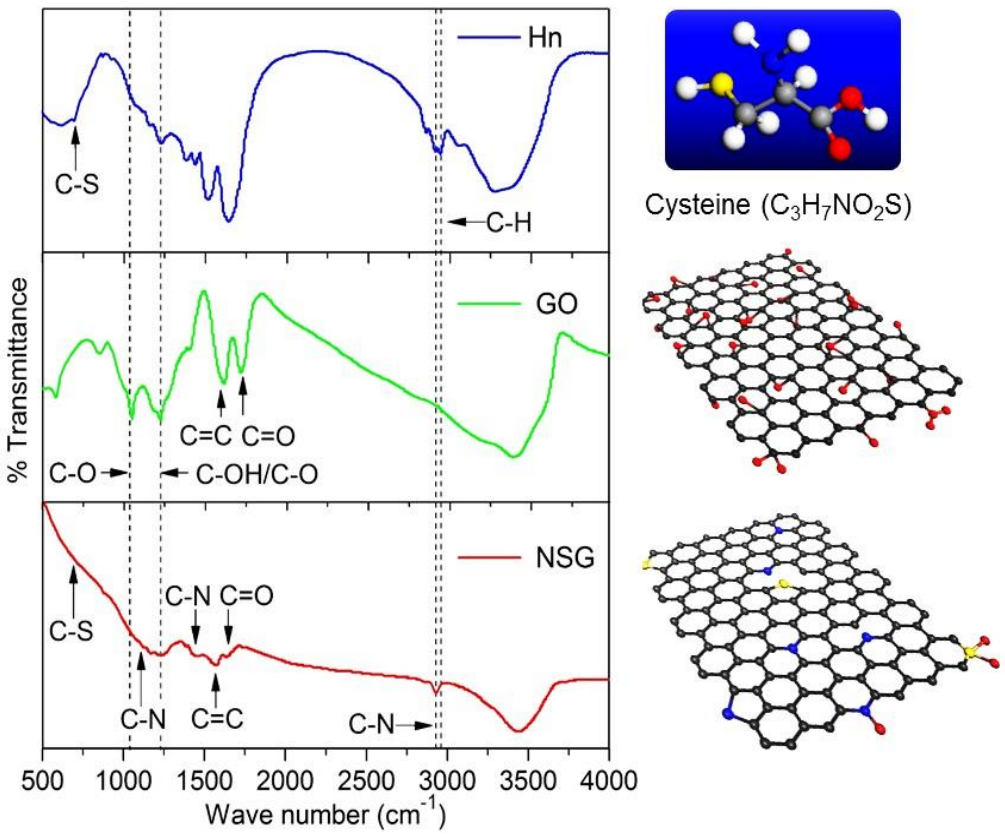

Figure S1 FT-IR spectra and corresponding illustration of main structural configuration of horn (Hn), GO, and NSG. The atoms are: C-gray, H-white, O-red, N-blue, S-yellow.

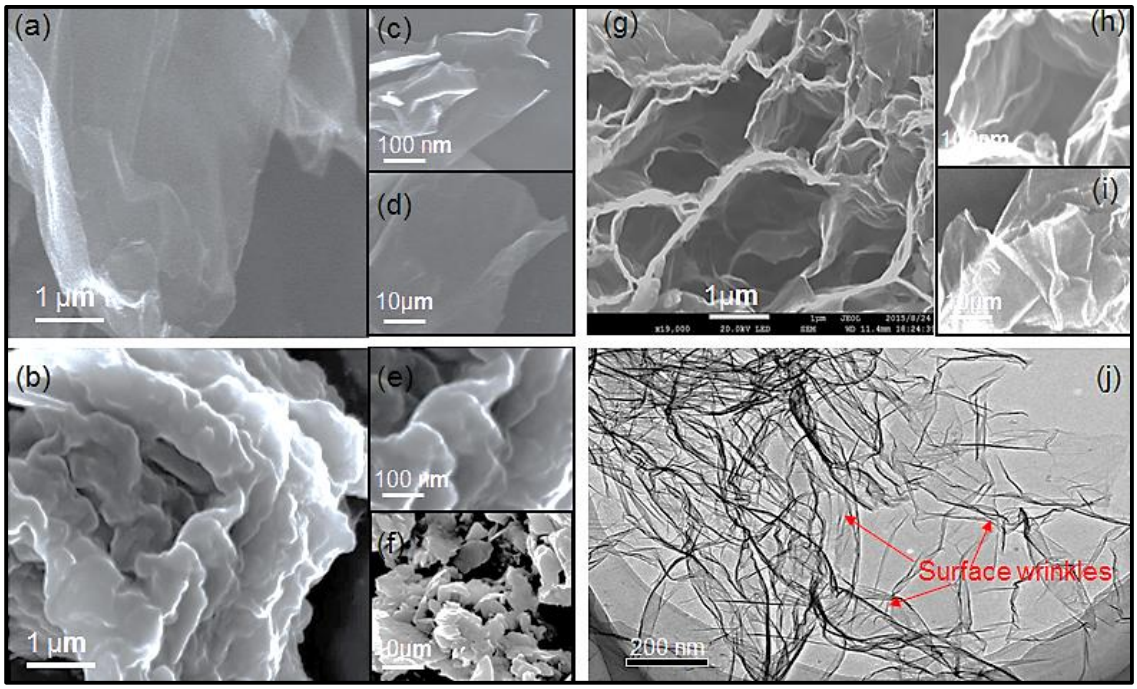

Figure S2 FE-SEM images of GO (a, c, d), horn (b, e, f), and NSG (g, h, i) at different magnification scales, and (j) TEM image of NSG.

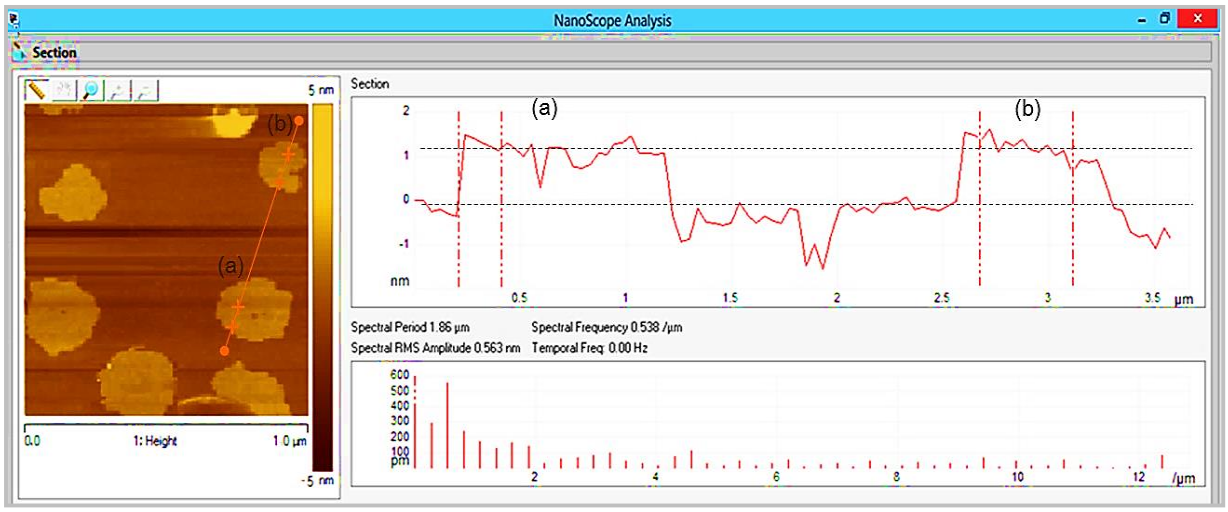

Figure S3 Atomic force micrograph (AFM) of graphene oxide and corresponding surface scan profiles. The approximated average sheet thickness is ~1.2 nm. The image was scanned on a Si tip NanoScope IIIA, Digital Instruments/VEECO in tapping mode, and processed with a NanoScope Analysis Software. Dash lines and cross marks are guide to eye.

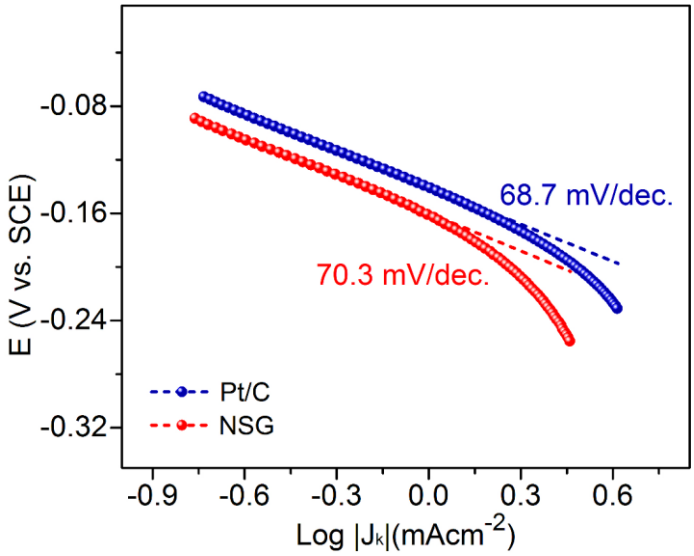

Figure S4 (a) Tafel plots of NSG and Pt/C catalysts in 0.1 M KOH.

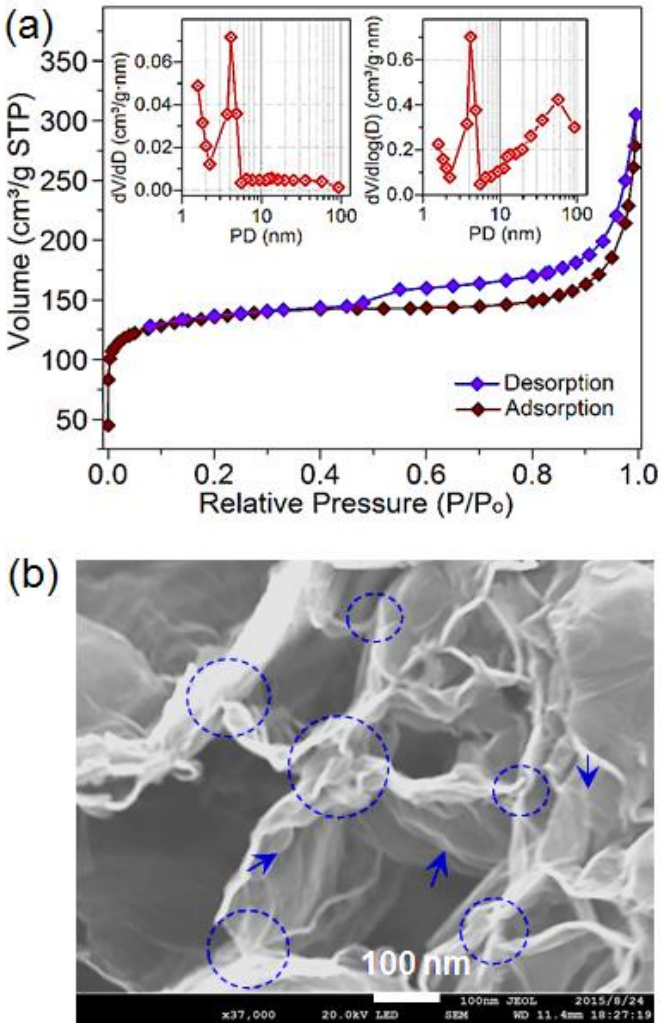

Figure S5 NSG (a) Nitrogen adsorption-desorption isotherm and pore size distribution profiles (inset), (b) SEM image. Dash circles show edge-to-edge linkage and arrows indicate surface wrinkles.

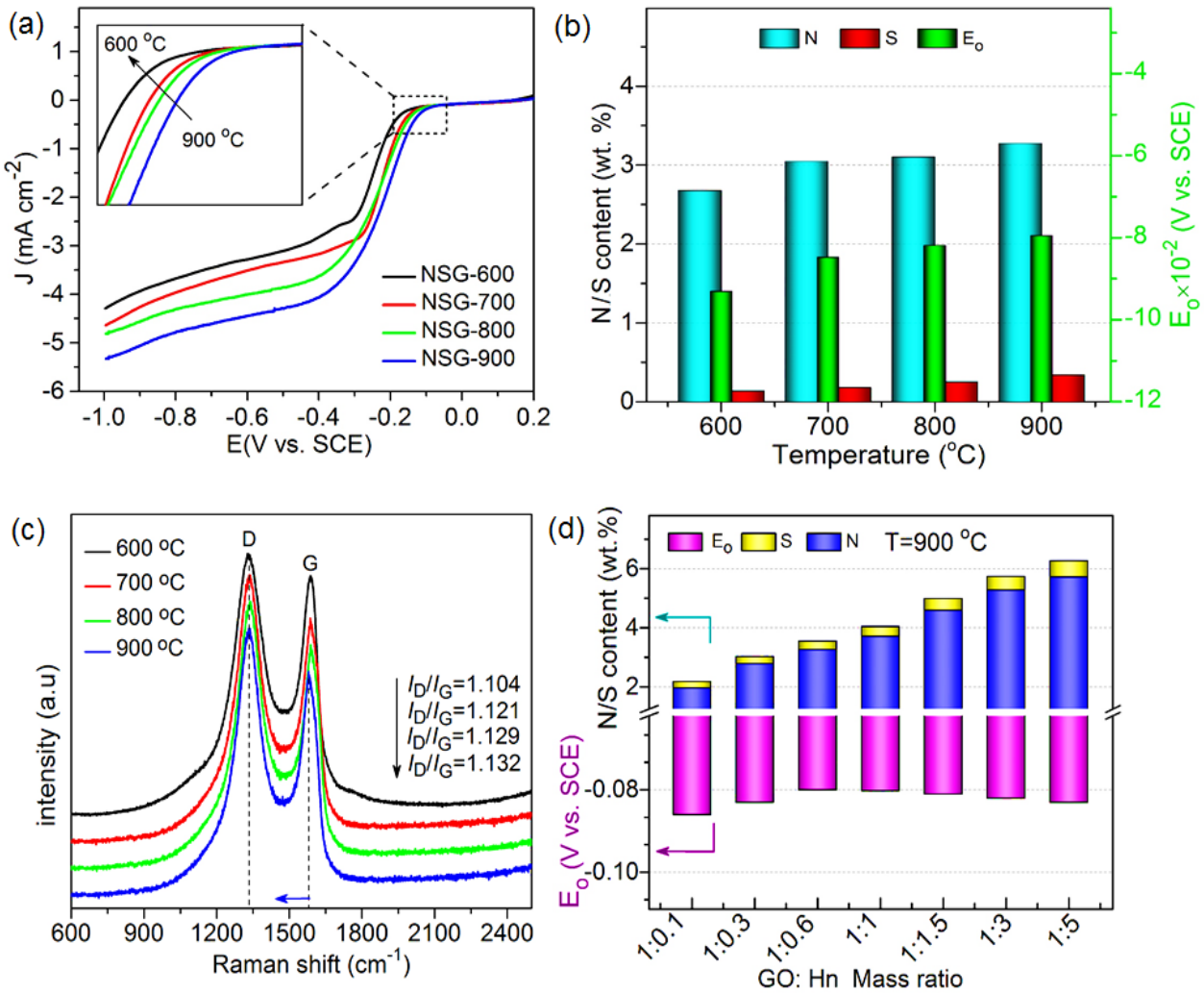

Figure S6 NSG catalyst prepared at various pyrolysis temperatures (a) LSV curves, (b) content of doped N and S, and corresponding E_o, (c) Raman spectra, (d) relative doping ratios and corresponding E_o at constant GO mass ratio and temperatures at 900 °C.

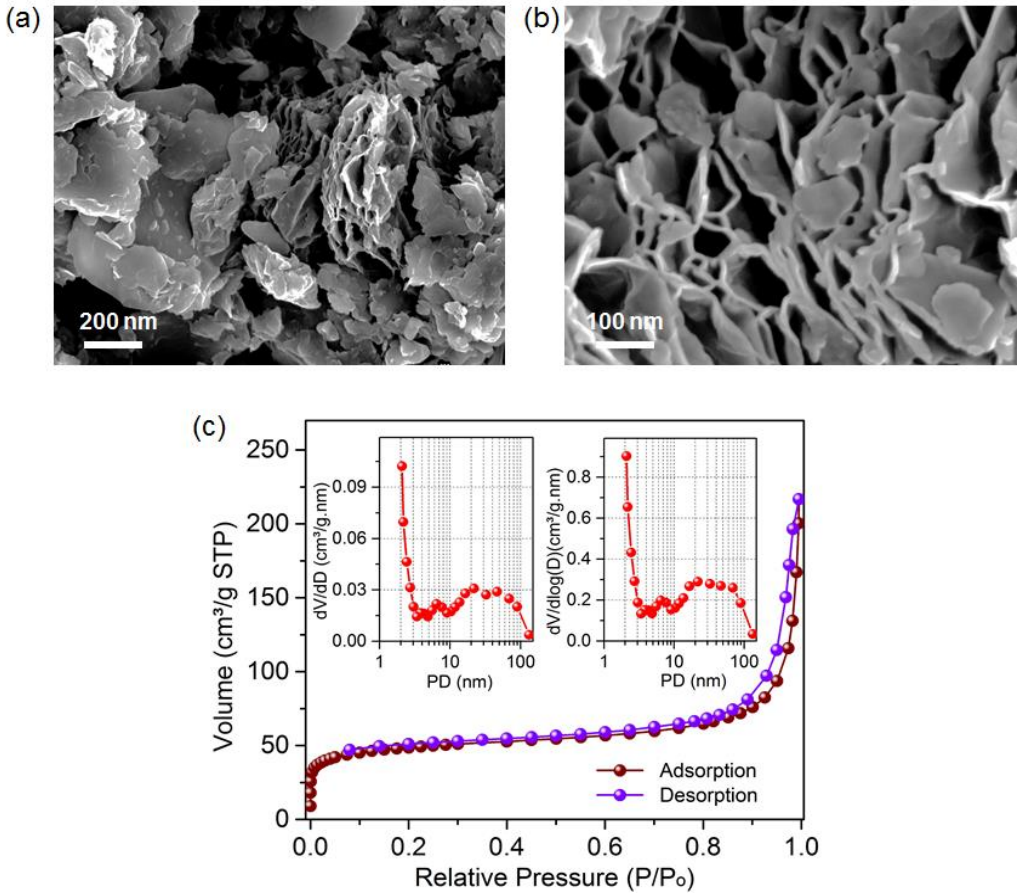

Figure S7 (a and b) SEM images, and (c) Nitrogen adsorption-desorption isotherm and pore size distribution profiles (inset) of NSG prepared at a high GO/Hn mass ratio of 1:5, respectively.

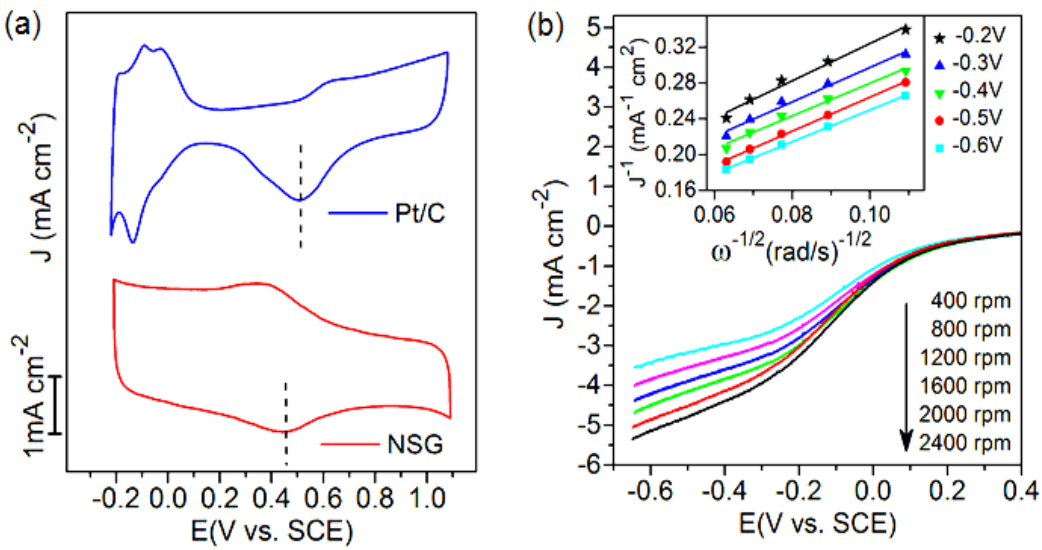

Figure S8 (a) CV curves of NSG and Pt/C, (b) LSV curves of NSG at different rotation rates, Inset is the corresponding K-L plots. Data were conducted in 0.1 M $HClO_4$ aqueous solution.

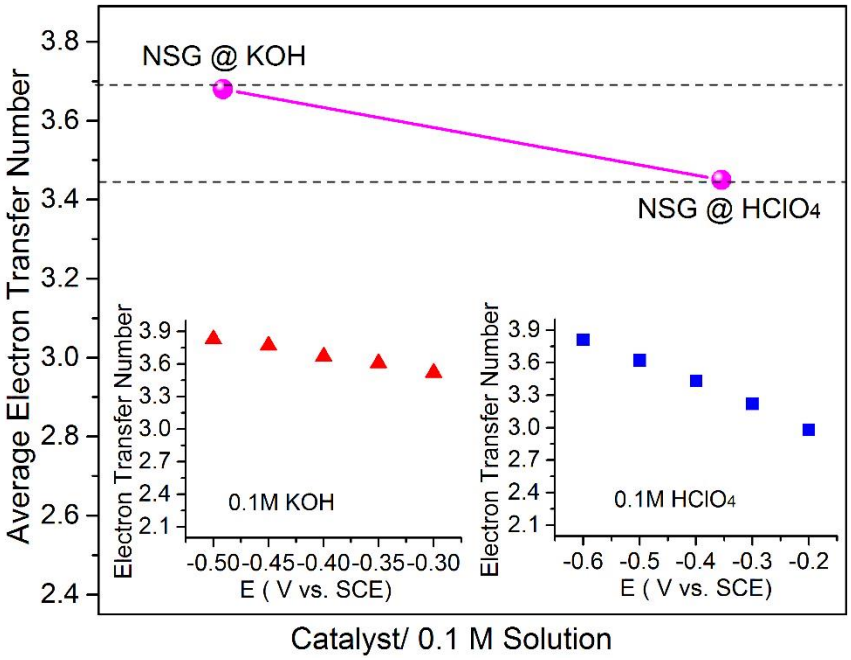

Figure S9 *Average* number of electrons transferred for oxygen reduction in alkaline (0.1M KOH) and acidic (0.1M $HClO_4$) media. An inset is the number of electrons transferred at various potentials under the electrolytes indicated in the figures.

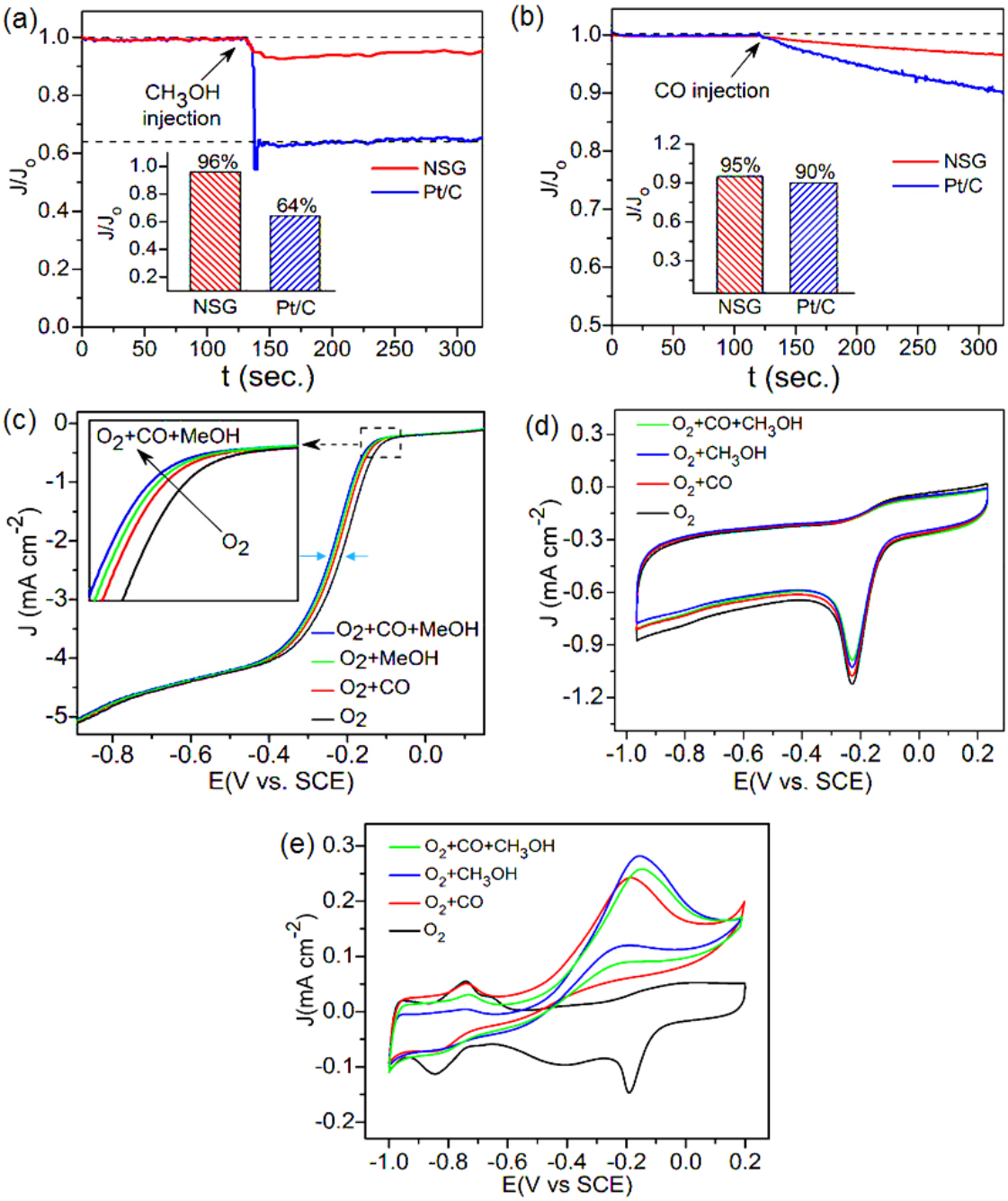

Figure S10 NSG catalyst tolerance by chronoamperometry (i-t) scan to (a) Methanol, and (b) CO, (An inset is the relative current retention after i-t scan), (c) LSV scan profiles, and (d) CV scan profiles of NSG, and (e) corresponding CV curves of Pt/C. Data were recorded in 0.1 M KOH solution under the condition indicated in the figure, $V_{CO}/V_{O2} \approx 10\%$, 1M CH_3OH, LSV at 1600 rpm.

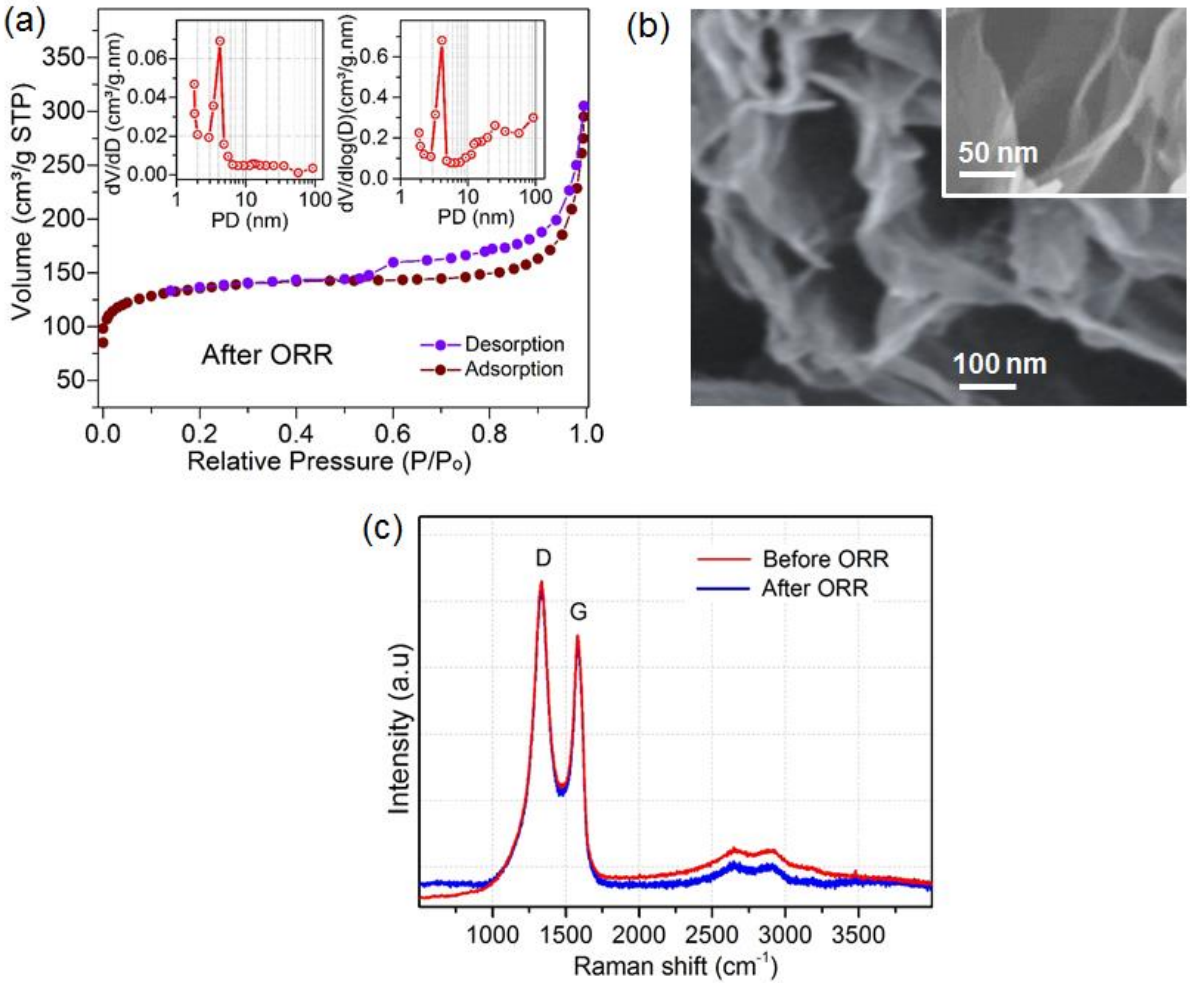

Figure S11 NSG (a) Nitrogen adsorption-desorption isotherm and pore size distribution (inset), (b) SEM images and (c) Raman spectra. Data were recorded after electrochemical tests (ORR, $CV_{10,000,}$ and i-$t_{10,000}$) in 0.1M KOH. Samples were thoroughly washed in ethanol, rinsed with copious amount of DI water after electrochemical tests, and dried at 80 ^{o}C for 12 h before characterization.

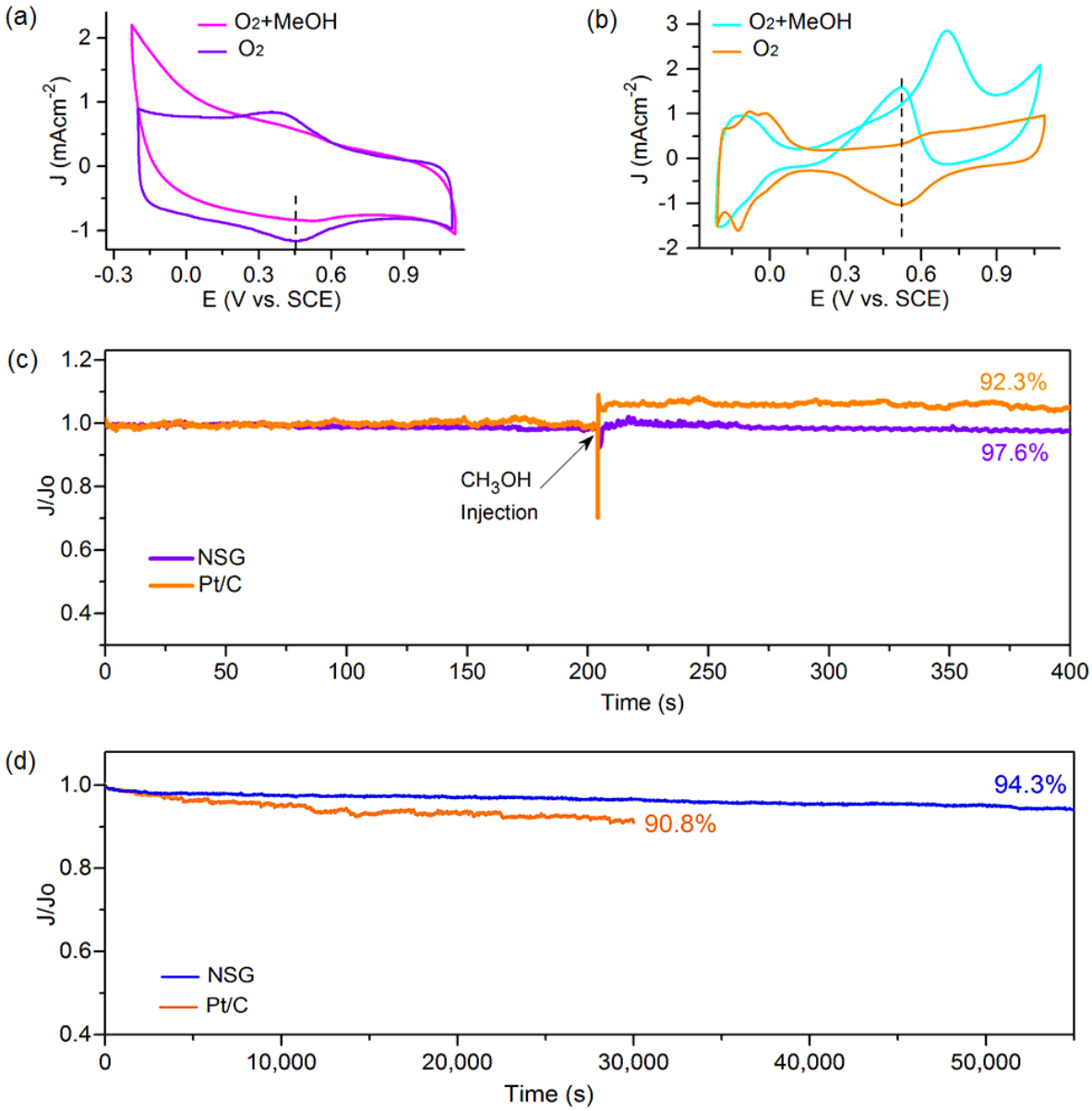

Figure S12 Methanol electrooxidation (a) CV curves of NSG in O_2-saturated electrolyte before and after methanol injection, (b) CV curves of Pt/C in O_2-saturated electrolyte before and after methanol injection. Chronoamperometry (i-t) scan profiles of NSG and Pt/C against (c) methanol oxidation and (d) time. All data were recorded in 0.1M $HClO_4$ aqueous solution.

Table S1 Elemental composition by carbon elemental analysis and XPS surface scan.

Element	Elemental Analysis (wt. %)				XPS (at. %)	
	GO	Hn	[a]HnGO	[b] NSG	[a]HnGO	[b] NSG
C	70.30	51.22	63.79	91.12	65.60	91.41
O	29.50	30.36	31.01	5.43	30.16	5.15
N	–	16.53	3.24	3.13	3.17	3.14
S	–	1.79	1.09	0.28	1.04	0.22

[a]Mixture of horn and GO before pyrolysis

[b]N, S co-doped graphene obtained after pyrolysis at 900 °C for 2h under Ar flow.

Table S2 Effects of temperature on the composition of NSG prepared with horn and high purity cysteine. All samples were obtained using a mass ratio of 1: 0.6.

Component	NSG (GO/Hn)				[a]NSG (GO/Hn)		[b]NSG (GO/L-cysteine)	
Temp./ °C	600	700	800	900	[a]700	[a]900	[b]700	[b]900
N	2.878	3.045	3.102	3.127	3.101	3.196	2.420	1.700
S	0.176	0.188	0.212	0.282	0.150	0.374	3.330	2.268
%Yield	32.61	31.64	30.81	26.35	30.88	27.04	22.69	20.35

[a]Indicates a repeated test with fresh NSG samples from a GO/Horn mixture.

[b]Indicates samples prepared from GO/pure cysteine mixture.

Mass of sample for elemental analysis (NSG: ~1.756 mg; [a]NSG: ~2.503 mg; [b]NSG: ~1.539 mg)

Table S3 Optical photograph of samples at various mass ratios before and after pyrolysis and their corresponding SEM images after pyrolysis.

GO/Hn mass ratio	Before pyrolysis (Raw mixture)	After Pyrolysis at 900 ºC	SEM Images (Scale: 100 nm)
1: **0.1**			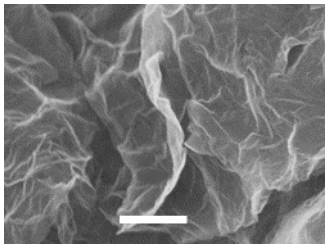
1: **0.6**			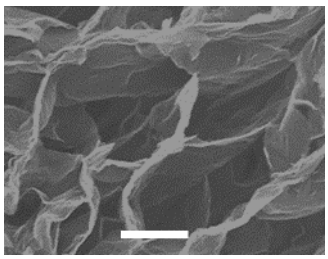
1: **1.5**			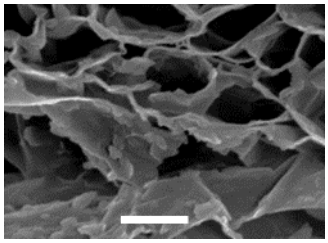
1: **5**			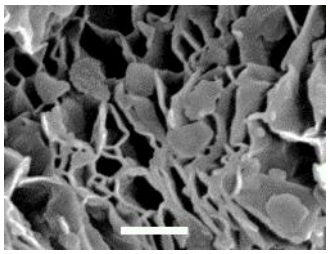
1: **0.6** GO/ L-Cysteine			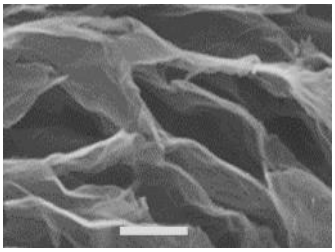

Table S4 Optical photograph of samples obtained before and after pyrolysis. GO/Hn mass ratio is 1: 0.6.

Temp./ ºC	Before pyrolysis	After Pyrolysis	Typical horn samples
600			
700			
800			

The optical images in **Table S3** clearly show a quantitative decrease of pyrolyzed samples as the GO/Hn mass ratio increases. With the increase in volume, the mass of pyrolyzed product drastically decreases, indicating the formation of aerogel structures with low density as temperature rises. With the same ratio and processing conditions, the sample obtained by using pure cysteine (^{b}NSG) yields the highest quantity by volume. **Table S4** also shows that with the increase in temperature, the quantity by volume, also increases suggesting that aerogel can be obtained at relatively higher temperatures and lower mass ratio. Also, from **Table S2**, it can be observed that the contents of both N and S decrease as the temperature increases for samples

obtained with GO/pure cysteine mixture contrary to that of GO/Hn. By using pure cysteine, the amount of doped S becomes higher than with the use of Hn but lower in N content, suggesting that other minor keratinous amino acid groups in horn may have contributed to the high content of N during the GO/Hn thermal reaction. As a verification, the test was repeated for GO/Hn using fresh samples prepared at 700 and 900 ^{o}C, which also show that both the N and S contents slightly increase as the temperature was raised from 700 to 900 ^{o}C. The reasons for this phenomena are discussed in the main text.

Table S5 A comparison of the ORR properties of N, S dual-doped Carbon Frameworks/Graphene in aqueous alkaline and acidic electrolytes.

Catalyst	Heteroatom source (at. %)		SS	ORR in 0.1M KOH			ORR in $HClO_4$			Ref.
	Nitrogen	Sulfur		E_p	$E_{1/2}$	n_a	E_p	j_L	n_a	
NSG	*Horn (3.14)	*Horn (0.22)	1	-0.22	-0.23	3.68	+0.45	-0.47	3.45	This work
GC-NLS	▪NH_3 (2.03)	▪Phenyl disulfide (0.23)	2	–	-0.24	3.8•	–	–	–	[1]
^{HT}SN/C-900	▪1-allyl-2-thiourea (7.2)	▪1-allyl-2 thiourea (1.6)	2	-0.34	-0.32	3.66	–	–	–	[2]
^{HT}NG/NS-900/	▪ NH_3 (4.6)	▪H_2S (1.25)	3	-0.36	<-3.0	3.20	–	–	–	[3]
^{HT}N-S-G	Melamine	▪Benzyl disulfide	3	-0.28	<-3.4	3.60•	–	–	–	[4]

GIL-carbon	▪[Bmim][Tf2N] and N_2 (13.02)	▪[Bmim][Tf2N] (13.02)	1	-0.26	-0.31	3.64	×	-5.20	3.16	[5]
NSGMCNs-1100	▪Thiourea (4.1)	▪Thiourea (2.2)	2	-0.27	-0.25	3.50	–	–	–	[6]
N/S-GFs	▪Thiourea (12.3)	▪Thiourea (18.4)	2	-0.32	-0.36	3.90•	–	–	–	[7]
N-S-G	▪Thiourea (3.2)	▪Thiourea (1.22)	1	-0.31	-0.32	3.91•	–	–	–	[8]
SN-rGO	▪Thiourea –	▪Thiourea/ Na_2S –	1	-0.40	-0.41	3.50	–	–	–	[9]
NS-CNTs	▪ NH_3 –	▪Toluenethiol /CS_2 –	2	-0.30	-0.23	4.00•	+0.29	-4.65	3.42	[10]
S_1N_2-GN	▪Pyridine-dipyrrolemethane (1.91)	▪Bithiophene dipyrrolemethane (2.63)	2	-0.27	-0.39	3.70	–	–	–	[11]
NS-G	▪ Hydrazine monohydrate –	▪2-Amino-thiophenol –	3	-0.26	-0.37	3.20	–	–	–	[12]
3D NG-900	▪Polypyrrole (2-3)	–	2	-0.26	-0.32	3.80•	–	–	–	[13]
PAC/5S	(6.55)	(9.52)	3	–	-0.21	3.82•	–	–	–	[14]
N/S-GP	▪3-amino benzene sulfonic acid –	▪3-amino benzene sulfonic acid –	2	-0.35	-0.37	3.94•	–	–	–	[15]
$^{HT}NOSC_8$-900	▪ $(NH_4)_2S_2O_8$	▪ $(NH_4)_2S_2O_8$	3	-0.21	-0.23	4.00•	–	–	–	[16]
FeNS-EGO	▪Pyrrole (3.4)	▪ $(NH_4)_2SO_4$ (4.1)	2	-0.24	-0.36	3.40	–	–	–	[17]
CSNP-900	▪$C_4H_{10}NO_3PS$ (1.83)	▪$C_4H_{10}NO_3PS$ (0.46)	2	-0.32	-0.38	2.99	–	–	–	[18]
N/S-G900	▪$C_8H_4NO_2$ 2.12	$C_3H_7NSO_2$ 1.70	3	-0.36	-0.34	3.36	–	–	–	[19]
SNDC	▪Dicyandiamide (7.58)	$C_3H_7NSO_2$ (0.57)	2	–	–	–	–	–	3.7•	[20]

^{HT}NS-MCV	▪Cyanamide (0.8)	▪Benzyldisulfide (0.52)	3	-0.29	-0.31	3.70•	–	–	–	[21]
^{HT}D-CNTs-MPC	▪Bi-CoPc /N_2 (4.97)	▪Bi-CoPc (2.51)	3	-0.30	-0.23	3.69	–	–	–	[22]
NSG	▪ [BSO_3Hmim] [HSO_4 (3.76)	▪ [BSO_3Hmim] [HSO_4] (0.36)	1	-0.35	-0.29	3.50•	–	–	–	[23]
CFO/NS-rGO	▪Thio-acetamide (1.32)	▪Thio-acetamide (3.14)	3	-0.32	-0.26	4.00•	–	–	–	[24]
NSCNT-3	▪Thiourea/N_2 (1.94)	▪Thiourea (1.52)	3	0.19	0.17	3.86•	–	–	–	[25]

Notes on table:

	Acronyms for catalysts are stated as used in the related references.
(SS)	Number of synthesis steps to achieve a dual heteroatom doped porous carbon framework.
(HT)	Hard-template used to achieve porosity, implying additional synthesis steps and cost.
(*)	Environmentally-friendly, easy access, and cheap heteroatom source.
(▪)	Chemical reagent as heteroatom source: relatively costly and potentially toxic.
(E_p)	Cathodic peak potential by cyclic voltammetry.
($E_{1/2}$)	Half-wave potential by linear sweep voltammetry
(j_L)	Limiting current density.
(n_a)	Average number of electrons transferred.
(●)	Electron transfer number was determined at a single potential (not the average).
(×)	Featureless cathodic peak by cyclic voltammetry in acidic media.
(–)	No experimental data provided.
(Ref.)	References.

Table S6 A comparison of OER oxidation and overall potentials of NSG with other materials

Catalyst	j (mA cm^{-2})	$E_{j=10}$ /V	Overall ΔE ($E_{j=10} - E_{1/2}$) /V	Ref.
NSG	10	0.69	0.92	This work
	5	0.60	0.83	
Pt/C	5	0.90	1.09	This work
N,S-CN	10	0.68	0.88	[26]
	5	0.65	0.85	
B-Graphene	5	0.90	1.13	[27]
NG-1000	2	0.80	1.00	[28]
PCN–CFP	10	0.61	0.96	[29]
CNT@NCNT	10	0.75	1.03	[30]
	5	0.67	0.95	
Mn_xO_y/NC	10	0.67	0.93	[31]
N-graphene/ CNT	10	1.63	1.00	[32]
Co_3O_4/NBGHSs	10	0.71	0.86	[33]
CaMn4Ox	10	0.81	1.04	[34]

Acronyms for catalysts are stated as used in the related references.

(Ref.) References.

REFERENCES

(1) Higgins, D. C.; Hoque, M. A.; Hassan, F.; Choi, J-Y.; Kim, B., and Chen, Z. Oxygen Reduction on Graphene–Carbon Nanotube Composites Doped Sequentially with Nitrogen and Sulfur. *ACS Catal*. **2014**, 4, 2734 – 2740.

(2) Li, Y.; Zhang, H.; Wang, Y.; Liu, P.; Yang, H.; Yao, X.; Wang, D.; Tang, Z.; and Zhao, H. A Self-Sponsored Doping Approach for Controllable Synthesis of S and N Co-Doped Trimodal-Porous Structured Graphitic Carbon Electrocatalysts. *Energy Environ. Sci.* **2014**, **7**, 3720–3726.

(3) Shubin, Y.; Zhi, L.; Tang, K.; Feng, X.; Maier, J.; and Müllen, K. Efficient Synthesis of Heteroatom (N or S)-Doped Graphene Based on Ultrathin Graphene Oxide-Porous Silica Sheets for Oxygen Reduction Reactions. *Adv. Funct. Mater.* **2012**, 22, 3634–3640.

(4) Liang, J.; Jiao, Y.; Jaroniec, M.; Qiao, S. Z. Sulfur and Nitrogen Dual-Doped Mesoporous Graphene Electrocatalyst for Oxygen Reduction with Synergistically Enhanced Performance. *Angew. Chem. Int. Ed.* **2012**, 51, 11496–11500.

(5) She, Y.; Lu, Z.; Ni, M.; Li, L.; and Leung, M. K. H. Facile Synthesis of Nitrogen and Sulfur Codoped Carbon from Ionic Liquid as Metal-Free Catalyst for Oxygen Reduction Reaction. *ACS Appl. Mater. Interfaces* **2015**, 13, 7214–7221.

(6) Chen, J.; Zhang, H.; Liu, P.; Li, Y.; Li, G.; An, T.; Zhao, H. Thiourea Sole Doping Reagent Approach for Controllable N, S Co-Doping of Pre-synthesized Large-Sized Carbon Nanospheres as Electrocatalyst for Oxygen Reduction Reaction. *Carbon* **2015**, 92, 339–347.

(7) Su, Y.; Zhang, Y.; Zhuang, X.; Li, S.; Wu, D.; Zhang, F.; Feng, X. Low-Temperature Synthesis of Nitrogen/Sulfur Co-doped Three-Dimensional Graphene Frameworks as Efficient Metal-Free Electrocatalyst for Oxygen Reduction Reaction. *Carbon* **2013**, 62, 296–301.

(8) Wang, X.; Wang, J.; Wang, D.; Dou, S.; Ma, Z.; Wu, J.; Tao, L.; Shen, A.; Ouyang, C.; Liu, Q.; Wang, S. One-Pot Synthesis of Nitrogen and Sulfur Co-doped Graphene as Efficient Metal-

Free Electrocatalysts for the Oxygen Reduction Reaction. *Chem. Commun*. **2014**, 50, 4839–42.

(9) Bag, S.; Mondal, B.; Das, A. K.; Raj, C. R. Nitrogen and Sulfur Dual-Doped Reduced Graphene Oxide: Synergistic Effect of Dopants towards Oxygen Reduction Reaction. *Electrochim. Acta* **2015**, 163, 16–23.

(10) Shi, Q.; Peng, F.; Liao, S.; Wang, H.; Yu, H.; Liu, Z.; Zhang, B.; and Su, D. Sulfur and Nitrogen Co-doped Carbon Nanotubes for Enhancing Electrochemical Oxygen Reduction Activity in Acidic and Alkaline Media. *J. Mater. Chem. A* **2013**, 1, 14853–4857.

(11) You, J. M.; Ahmed, M. S.; Han, H. S.; Choe, J. E.; Üstündag, Z.; Jeon, S. New Approach of Nitrogen and Sulfur-Doped Graphene Synthesis using Dipyrrolemethane and their Electrocatalytic Activity for Oxygen Reduction in Alkaline Media. *J. Power Sources* **2015**, 275, 73–79.

(12) Ai, W.; Luo, Z.; Jiang, J.; Zhu, J.; Du, Z.; Fan, Z.; Xie, L.; Zhang, H.; Huang, W.; and Yu, T. Nitrogen and Sulfur Codoped Graphene: Multifunctional Electrode Materials for High-Performance Li-ion Batteries and Oxygen Reduction Reaction. *Adv. Mater*. **2014**, 26, 6186–6192.

(13) Lin, Z.; Waller, G. H.; Liu, Y.; Liu, M.; Wong, C.-P. 3D Nitrogen-Doped Graphene Prepared by Pyrolysis of Graphene Oxide with Polypyrrole for Electrocatalysis of Oxygen Reduction Reaction. *Nano Energy* **2013**, 2, 241–248.

(14) You, C.; Liao, S.; Li, H.; Hou, S.; Peng, H.; Zeng, X.; Liu, F.; Zheng, R.; Fu, Z.; Li, Y. Uniform Nitrogen and Sulfur Co-doped Carbon Nanospheres as Catalysts for the Oxygen Reduction Reaction. *Carbon* **2014**, 69, 294–301.

(15) Akhter, T.; Islam, M. M.; Faisal, S. N.; Haque, E.; Minett, A. I.; Liu, H. K.; Konstantinov, K.; and Dou, S. X. Akhter, T., Islam, M.M., Faisal, S.N., Haque, E., Minett, A.I., Liu, H.K., Konstantinov, K.; and Dou, S.X. Self-Assembled N/S Codoped Flexible Graphene Paper for High Performance Energy Storage and Oxygen Reduction Reaction. *ACS Appl. Mater. Interfaces* **2016**, 8, 2078–2087.

(16) Meng, Y.; Voiry, D.; Goswami, A.; Zou, X.; Huang, X.; Chhowalla, M.; Liu, Z.; and Asefa, T. N-, O-, and S-Tridoped Nanoporous Carbons as Selective Catalysts for Oxygen Reduction and Alcohol Oxidation Reactions. *J. Am. Chem. Soc*. **2014**, 136, 13554–13557.

(17) Parvez, K.; RincÓn, R. A.; Weber, N.-E.; Cha, K. C.; and Venkataraman, S. S. One-Step Electrochemical Synthesis of Nitrogen and Sulfur Co-Doped High-Quality Graphene Oxide. *Chem. Commun*. **2016**, 52, 5714–5717.

(18) Dou, S., Shen, A.; Ma, Z.; Wu, J.; Tao, L.; Wang, S. N-, P-and S-Tridoped Graphene as Metal-Free Electrocatalyst for Oxygen Reduction Reaction. *J. Electroanal. Chem.* **2015**, 753, 21–27.

(19) Zhang, H.; Liu, X.; He, G.; Zhang, X.; Bao, S.; Hu, W. Bioinspired Synthesis of Nitrogen/Sulfur Co-doped Graphene as an Efficient Electrocatalyst for Oxygen Reduction Reaction. *J. Power Sources* **2015**, 279, 252–258.

(20) Choi, C. H.; Chung, M. W.; Park, S. H.; and Woo, S. I. Additional Doping of Phosphorus and/or Sulfur into Nitrogen-Doped Carbon For Efficient Oxygen Reduction Reaction in Acidic Media. *Phys. Chem. Chem. Phys*. **2013**, 15, 1802–1805.

(21) Han, C.; Bo, X.; Zhang, Y.; Li, M.; Guo, L. One-Pot Synthesis of Nitrogen and Sulfur Co-doped Onion-Like Mesoporous Carbon Vesicle as an Efficient Metal-Free Catalyst for Oxygen Reduction Reaction in Alkaline Solution. *J. Power Sources* **2014**, 272, 267–276.

(22) Nie, R.; Bo, X.; Luhana, C.; Nsabimana, A.; Guo, L. Simultaneous Formation of Nitrogen and Sulfur-Doped Carbon Nanotubes-Mesoporous Carbon and its Electrocatalytic Activity for Oxygen Reduction Reaction. *Int. J. Hydrogen Energy* **2014**, 39, 12597–12603.

(23) Ma, R.; Xia, B. Y.; Zhou, Y.; Li, P.; Chen, Y.; Liu, Q.; Wang, J. Ionic Liquid-Assisted Synthesis of Dual-Doped Graphene as Efficient Electrocatalysts for Oxygen Reduction. *Carbon* **2016**, 102, 58–65.

(24) Yan, W.; Cao, X.; Tian, J.; Jin, C.; Ke, K.; and Yang, R. Nitrogen/Sulfur Dual-doped 3D

Reduced Graphene Oxide Networks-Supported $CoFe_2O_4$ with Enhanced Electrocatalytic Activities for Oxygen Reduction and Evolution Reactions. *Carbon* **2016**, 99, 195–202.

(25) Wang, J.; Wu, Z.; Han, L.; Lin, R.; Xiao, W.; Xuan, C.; Xin, H. L.; and Wang, D. Nitrogen and Sulfur Co-doping of Partially Exfoliated MWCNTS as 3-D Structured Electrocatalysts for the Oxygen Reduction Reaction. *J. Mater. Chem. A* **2016**, 4, 5678–5684.

(26) Qu, K.; Zheng, Y.; Dai, S.; Qiao, S. Z. Graphene Oxide-Polydopamine Derived N, S-Codoped Carbon Nanosheets as Superior Bifunctional Electrocatalysts for Oxygen Reduction and Evolution. *Nano Energy* **2016**, 19, 373–381.

(27) Vineesh, T. V.; Kumar, M. P.; Takahashi, C.; Kalita, G.; Alwarappan, S.; Pattanayak, D. K.; Narayanan, T. N. Activity of Boron-Doped Graphene Derived from Boron Carbide. *Adv. Energy Mater.* **2015**, 1500658, 1–8.

(28) Lin, Z.; Waller, G. H.; Liu, Y.; Liu, M.; Wong, C.-P. Simple Preparation of Nanoporous Few-Layer Nitrogen-Doped Graphene for use as an Efficient Electrocatalyst for Oxygen Reduction and Oxygen Evolution Reactions. *Carbon* **2013**, 53, 130–136.

(29) Ma, T.Y.; Ran, J.; Dai, S.; Jaroniec, M.; and Qiao, S. Z. Phosphorus-Doped Graphitic Carbon Nitrides Grown in Situ on Carbon-Fiber Paper: Flexible and Reversible Oxygen Electrodes. *Angew. Chem. Int. Ed.* **2015**, 54. 4646–4650.

(30) Tian, G. L.; Zhang, Q.; Zhang, B.; Jin, Y. G.; Huang, J. Q.; Su, D. S.; and Wei, F. Toward Full Exposure of "Active Sites": Nanocarbon Electrocatalyst with Surface Enriched Nitrogen for Superior Oxygen Reduction and Evolution Reactivity. *Adv. Funct. Mater.* **2014**, 24, 5956–5961.

(31) Masa, J.; Xia, W.; Sinev, I.; Zhao, A.; Sun, Z.; Grützke, S.; Weide, P.; Muhler, M.; and Schuhmann, W. Mn_xO_y/NC and Co_xO_y/NC Nanoparticles Embedded in a Nitrogen-Doped Carbon Matrix for High-Performance Bifunctional Oxygen Electrodes. *Angew. Chem. Int. Ed.* **2014**, *53*, 8508–8512.

(32) Tian, G. L.; Zhao, M. Q.; Yu, D.; Kong, X. Y.; Huang, J. Q.; Zhang, Q.; and Wei, F. Nitrogen-Doped Graphene/Carbon Nanotube Hybrids: In Situ Formation on Bifunctional Catalysts and their Superior Electrocatalytic Activity for Oxygen Evolution/Reduction Reaction. *Small* **2014**, 10, 2251–2259.

(33) Jiang, Z.; Jiang, Z.-J.; Maiyalagan, T.; and Manthiram, A. Cobalt Oxide-Coated N-and B-Doped Graphene Hollow Spheres as Bifunctional Electrocatalysts for Oxygen Reduction and Oxygen Evolution Reactions. *J. Mater. Chem. A* **2016**, 4, 5877–5889.

(34) Gorlin, Y.; Jaramillo, T.F. A Bifunctional Nonprecious Metal Catalyst for Oxygen Reduction and Water Oxidation. *J. Am. Chem. Soc*. **2010**, 132, 13612–13614.